Scripta Materialia 155 (2018) 16–20

Contents lists available at ScienceDirect

Scripta Materialia

journal homepage: www.elsevier.com/locate/scriptamat

Regular article

# Signatures of the unique microstructure of additively manufactured steel observed via diffraction

R. Pokharel [a,*], L. Balogh [b], D.W. Brown [a], B. Clausen [a], G.T. Gray III [a], V. Livescu [a], S.C. Vogel [a], S. Takajo [a,c]

[a] Los Alamos National Laboratory, Los Alamos, NM 87544, USA
[b] Queen's University, Kingston, Ontario K7L 3N6, Canada
[c] JFE Steel Corporation, Kurashiki 712, Japan

ARTICLE INFO

*Article history:*
Received 13 April 2018
Received in revised form 31 May 2018
Accepted 2 June 2018
Available online xxxx

*Keywords:*
Additive manufacturing
304 L stainless-steel
Microstructure
Dislocations
Neutron diffraction

ABSTRACT

A series of measurements were designed to gain confidence in the interpretation of the peak breadth in diffraction patterns collected from additively manufactured material, which has a novel microstructure in comparison to the well understood microstructure of wrought materials. Stainless steels made with two additive manufacturing techniques were compared to wrought material. Similar patterns observed in the scattering vector dependence for additively manufactured and deformed wrought materials suggested that the broadening in both materials was related to dislocations. This was confirmed by heat-treatment, during which both materials exhibited recovery due to the annealing of dislocations at the same temperature.



Metal additive manufacturing (AM) has the potential to be a disruptive technology by producing complex engineering components with reduced cost and waste [1–4] that simply cannot be made with conventional techniques [5, 6]. AM materials exhibit unique microstructures such as high dislocation density, secondary phases, tortuous grain morphology as well as chemical segregation resulting in material properties that significantly deviate from traditional wrought/cast materials [7–12]. The AM process exhibits similarity to welding in that both processes utilize a localized heat source to melt material producing refined grain-structure, directional grain-growth, and secondary phases in the fusion zone [4, 14–16]. However, there are two major distinction between the two processes. Welding is a joining process in which two finished parts with homogeneous microstructure are fused by a heat source traveling a relatively simple path to produce a final component. Deviant mechanical properties of the weld and heat affected zone resulting from the recast microstructure can be mitigated by design, for example, by added material near the joint as they are localized. In contrast, AM processes produce high-resolution near net-shape single component with complex geometry and heterogeneous local microstructure made by heat sources with complex paths including several thousand (millions) passes, corners, acceleration/deceleration, etc. This results in a locally more complex thermal profiles and heat conduction/convection that are distinct from that observed in welding [4, 15, 16]. Moreover, inherent build defects in AM material such as local porosity due to keyholing, residual stresses, local plasticity, surface roughness, and scan strategy dependent solidification texture influence the mechanical properties of the entire AM component [1–4] and thus cannot be shielded by design strategy. These effects are ubiquitous across AM builds and pose significant challenges for metal additive manufacturing.

Non-destructive nature of neutron diffraction (ND) measurements enables evolutionary characterization of bulk microstructures (several cm) at various stages of processing. Relatively high resolution neutron diffractometers can determine lattice parameters accurately enough to infer internal stresses, dislocation densities semi-quantitatively but with higher accuracy than TEM [17], provide phase fractions and texture information, all of which are impacted by the AM processing and, in turn, control mechanical properties. Past work has demonstrated signatures in diffraction patterns collected during annealing that herald the initiation of recovery (decrease in diffraction peak-breadth [18]) and recrystallization (rapid texture evolution [19]). Finally, as this work focuses on deformation and heat-treating properties, the time scale of ND measurements (minutes) matches well the kinetics of the processes.

All samples utilized in this study were prepared from the AISI-304 L-grade stainless-steel (SS). AM materials were fabricated via laser-based Powder-Bed-Fusion (PBF) and High-Power-Laser-Engineered-Net-Shaping (HPLENS) techniques [2]. Details of the fabrication techniques, microstructure characterization, and strength of the AM [8, 10] and baseline wrought materials [10] are presented elsewhere. ND data was collected in-situ during heating/cooling of PBF and HPLENS steels as well as as-received and deformed wrought 304 L-SS for comparison.

* Corresponding author.
*E-mail address:* reeju@lanl.gov (R. Pokharel).

https://doi.org/10.1016/j.scriptamat.2018.06.008
1359-6462/

This comparison to well understood processes in wrought material was carried out to develop an understanding and interpretation of diffraction data generated from AM stainless-steel. Specifically, AM materials contain several unique microstructural features, such as chemical segregation [11, 12] and large internal stresses, which could easily confound interpretation of diffraction-line-profile data.

High-resolution ND measurements were performed utilizing the SMARTS diffractometer and texture data were collected on the HIPPO diffractometer at the Lujan Center at LANSCE. Details of SMARTS [20] and HIPPO [21] are available elsewhere. The in-situ heating measurements were completed utilizing the $+90^{\circ}$ detector bank on SMARTS with relatively high temporal and moderately high peak resolutions (Full-Width-at-Half-Maximum (FWHM) ~0.5%), enabling the monitoring of individual peak-breadths and intensities to characterize the evolution of microstructure during imposed thermal cycles. Both deformed wrought and AM samples were heated from room-temperature (RT) to ~1200 K and cooled back to RT at 10 K/min and 2 K/min, respectively; while continuously recording diffraction patterns with a two-minute integration time. The high-resolution data (FWHM ~ 0.1%) for diffraction-line-profile-analysis were collected in the backscattering (153°) detector bank on SMARTS. The count-time for the line-profile measurements was 6 h, as much of the information is contained in the tails of the diffraction peaks, needing data with a high signal-noise ratio. The wrought material was not measured after heating due to limited available beamtime. Single-peak-fit analysis was performed with a pseudo-Voigt peak profile function in GSAS [22] automated by the SMARTsware program [23]. Quantitative line profile analysis was completed using the eCMWP software [24]. Texture analysis was performed following procedures in [25].

Fig. 1(a) shows diffraction patterns collected at room temperature from as-received and deformed wrought 304 L-SS samples. Fig. 1 (b) shows diffraction patterns collected from the as-built PBF sample before and after heat-treatment to 1200 K for 1 h. The insets on both plots show the expanded view of the normalized (200) peaks in four conditions. The unindexed peaks are from sample holders and furnace setup. Several features are apparent when comparing the evolution of diffraction patterns. Peak intensity changes which are *hkl* dependent are evident in the diffraction patterns collected from the wrought material before and after deformation. These are manifestations of the known texture changes in the material associated with compression [26–28] of this face-centered-cubic (fcc) alloy.

Also apparent are large changes in the diffraction peak-breadth. The deformed wrought material exhibits broader peaks in comparison to the as-received wrought material. In wrought SS, the increase in peak-breadth with deformation is well understood to be associated with an increase of dislocation density in the material [24, 29, 30]. Other, possible confounding microstructure features such as chemical segregation (leading to peak broadening due to gradients in chemical strain) or small crystallite size (leading to particle size broadening) are not present given the relatively small plastic strain (11%) enforced here.

Examination of the diffractions patterns from as-built and heat-treated AM materials shows comparable evolution although in the opposite sense than the compressed wrought 304 L-SS. Relative to those observed in the wrought material, very small changes in peak intensity are observed between as-built and heat-treated AM materials (Fig. 1). However, comparable changes in peak-breadth are evident. The diffraction peaks from the as-built AM materials are very broad and significantly narrows following heat-treatment.

Fig. 2(a) shows conventional Williamson-Hall (WH) [31] plots generated from the high-resolution data collected on SMARTS from wrought material before and after deformation, and as-built AM materials. The instrumental resolution as determined by a $CaF_2$ calibrant was subtracted in quadrature, thus only sample broadening is displayed [32]. Peak-widths (ΔQ) from 12 peaks from 304 L-SS are shown as a function of the scattering vector Q. In the wrought material, a significant increase of the peak-breadth is observed following 11% compression, where the only microstructural change should be an increase in dislocation density. Moreover, the apparent scatter in the peak-breadth data is not noise but the signature of strain anisotropy, well understood phenomena associated with the contrast-factors of dislocations as a function of *hkl* [33].

Fig. 2(b) shows the modified-WH plot in which strain anisotropy, the non-monotonous dependence of peak broadening as a function of Q, is accounted for by the average contrast-factors for individual

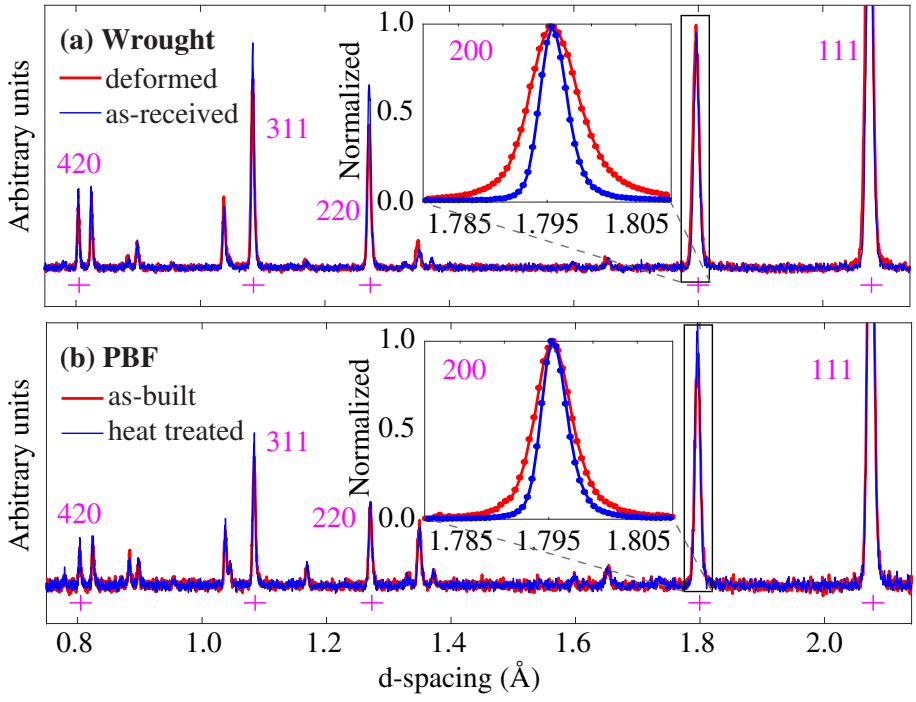


**Fig. 1.** Raw diffraction profiles. (a) Wrought and wrought deformed samples. (b) PBF and PBF annealed samples. The insets show the expanded view of 200 austenite peaks in the four samples. Note the remnant peaks are from sample holders and furnace setup.